

GLOBAL JOURNAL OF ENGINEERING SCIENCE AND RESEARCHES

MOLECULAR STRUCTURE, FIRST ORDER HYPERPOLARIZABILITY, HOMO AND LUMO ANALYSIS, MEP AND NBO ANALYSIS OF MONOHYDROXYMETHYL-TTFSBY DENSITY FUNCTIONAL THEORY

Amel Bendjeddou^{*1}, Tahar Abbaz², Abdelkrim Gouasmia³ and Didier Villemin⁴

^{*1&2}Laboratory of Aquatic and Terrestrial Ecosystems, Org. and Bioorg. Chem. Group, University of Mohamed-Cherif Messaadia, Souk Ahras, 41000, Algeria

^{2&3}Laboratory of Organic Materials and Heterochemistry, University of Larbi Tebessi, Tebessa, 12000, Algeria

⁴Laboratory of Molecular and Thio-Organic Chemistry, UMR CNRS 6507, INC3M, FR 3038, Labex EMC3, ensicaen & University of Caen, Caen 14050, France

ABSTRACT

To our knowledge, the theoretical calculations of monohydroxymethyl-TTFs **4a-d** have not been reported except in our work. Organic molecule containing extended π -conjugated electrons have characterized by large values of molecular first hyperpolarizabilities show enhanced NLO properties. Monohydroxymethyl-TTFsmolecules can show large first order hyperpolarizabilities (β) related to an electronic intra-molecular charge-transfer excitation between the ground and excited states. The redistribution of electron density (ED) in various bonding, antibonding orbitals and E(2) energies have been calculated by natural bond orbital (NBO) analysis and natural localized molecular orbital interactions to give clear evidence of stabilization originating from the hyperconjugation of various intra-molecular interactions.

Keywords- *Tetrathiafulvalenes, density functional theory, computational chemistry, electronic structure, quantum chemical calculations*

I. INTRODUCTION

Tetrathiafulvalene (TTF) and its derivatives are well-known as π electron-donor materials in the field of organic conductors [1]. As a result of progress in synthetic TTF chemistry, TTFs have been incorporated into a number of macrocyclic, molecular, and supramolecular systems in order to create multifunctional materials with desired structures, stability, and physical properties [1-3]. Therefore, considerable efforts are currently devoted to the modification of the TTF core with substituents such as pyridine-type heterocycles [4], acetylacetones [5], and phosphines [6], all of which are well tailored for a chelating coordination function toward various transition metal ions. On the other hand, TTFs are frequently used as donor units in donor-acceptor (D-A) ensembles, which are of considerable research interest due to their potential applications in sensors, optoelectronics, and molecular devices [3,7].

Nonlinear optical (NLO) materials have been attractive in recent years with respect to their future potential applications in the field of optoelectronic such as optical communication, optical computing, optical switching, and dynamic image processing [8,9]. Because of their high-molecular hyperpolarizabilities, organic materials display a number of significant NLO properties [10]. Organic materials have been of particular interest because the nonlinear optical response in this broad class of materials is microscopic in origin, offering an opportunity to use theoretical modeling coupled with synthetic flexibility to design and produce novel materials [11-13]. Also, organic nonlinear optical materials are attracting a great deal of attention, as they have large optical susceptibilities, inherent ultrafast response times, and high optical thresholds for laser power as compared with inorganic materials [14]. Experimental measurements and theoretical calculations on molecular first hyperpolarizability become one of the key factors in the second-order NLO materials design [15,16]. Theoretical determination of hyperpolarizability is quite useful both in understanding the relationship between the molecular structure and nonlinear optical properties [17]. It also provides a guideline to experimentalists for the design and synthesis of organic NLO materials [18,19].

In this work we have analyzed the molecular reactivity of series of monohydroxymethyl-TTFs through global and local reactivity descriptors derived from the Density Functional Theory (DFT). We consider that this kind of study will contribute to get a better understanding of the chemical behavior of the title compounds.

II. METHOD & MATERIAL

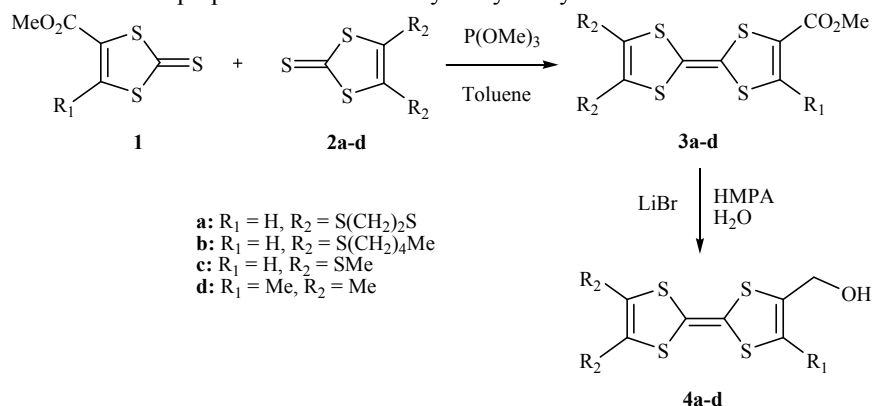
All computational calculations have been performed on personal computer using the Gaussian 09W program packages developed by Frisch and coworkers. The Becke's three parameter hybrid functional using the LYP correlation functional (B3LYP), one of the most robust functional of the hybrid family, was herein used for all the calculations, with 6.31G(d,p) basis set. Gaussian output files were visualized by means of GAUSSIAN VIEW 05 software.

III. RESULTS AND DISCUSSION

Chemistry

In a previous work [20], we have explained the synthesis of 2-monohydroxymethyl-TTFs **4a-d** indicated in Scheme 1. The starting mono esters **3** [21] were prepared by coupling the two corresponding 2-thio-1,3-dithioles using P(OMe)₃ with the following yields : in the case of **3a-d**, 62% starting from **1** and **2a**, 73% starting from **1** and **2b**, 81% starting from **1** and **3c**, and 68% starting from **1** and **2d**. The 2-monohydroxymethyl-TTFs **4a-d** were better prepared by decarbomethoxylation of mono esters **3a-d** by using LiBr-HMPA-H₂O [22-24] With yields: **4a** (60%), **4b** (83%), **4c** (85%) and **4d** (65%) after they were purified by column chromatography on silica gel.

Scheme 1. Synthetic route for the preparation of 2-monohydroxymethyl-TTFs **4a-d**



Molecular Geometry

The optimized molecular structure of the isolated monohydroxymethyl-TTFs **4a-d** are calculated using DFT theory at 6-31G(d,p) level. Figure 1 shows the optimized structure of compounds **4a-d** obtained from B3LYP methods, (atom numbering scheme adopted in the study). The optimized geometrical parameters are given in Table 1. The internal coordinates describe the position of the atoms in terms of distances, angles and dihedral angles with respect to an origin atom. The calculations converge to optimized geometries, which correspond to true energy minima, as revealed by the lack of imaginary frequencies in the vibrational mode calculation. Calculated geometric parameters represent a good approximation, and they are the base for calculating other parameters.

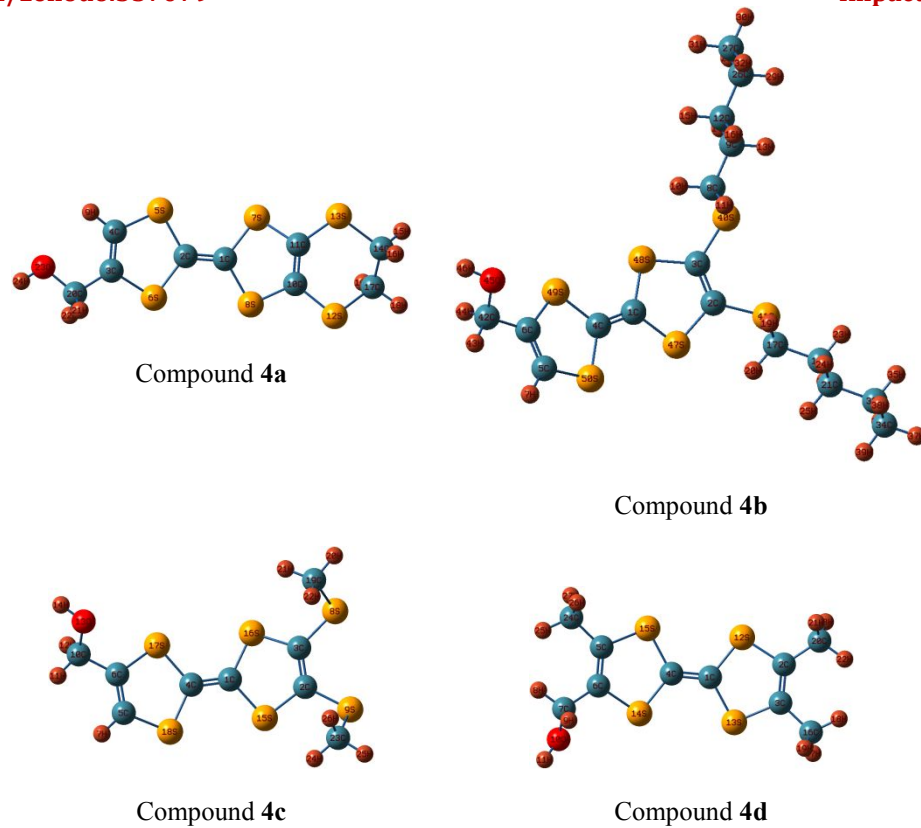


Figure 1. Optimized molecular structure of monohydroxymethyl-TTFs *4a-d*

Table 1. Optimized geometric parameters of compound *4a*

Bond Length(Å)	Bond Angles (°)		Dihedral Angles (°)	
R(1,2)	1.351	A(2,1,7)	123.504	D(7,1,2,6)
R(1,7)	1.783	A(2,1,8)	123.903	D(2,1,7,11)
R(1,8)	1.781	A(7,1,8)	112.578	D(1,2,6,3)
R(3,4)	1.337	A(1,2,5)	123.535	D(9,4,5,2)
R(3,20)	1.504	A(1,2,6)	122.937	D(1,7,11,10)
R(4,5)	1.762	A(5,2,6)	113.515	D(1,8,10,12)
R(4,9)	1.082	A(2,5,4)	94.652	D(8,10,11,7)
R(7,11)	1.785	A(2,6,3)	94.816	D(12,10,11,7)
R(10,12)	1.763	A(1,7,11)	93.529	D(8,10,12,17)
R(11,13)	1.764	A(1,8,10)	93.453	D(11,13,14,15)
R(14,17)	1.521	A(10,12,17)	96.354	D(11,13,14,17)
R(17,18)	1.094	A(11,13,14)	103.851	D(13,14,17,19)
R(20,21)	1.102	A(13,14,15)	105.965	D(15,14,17,18)
R(20,23)	1.417	A(15,14,16)	108.842	D(16,14,17,12)
R(23,24)	0.965	A(20,23,24)	107.928	D(22,20,23,24)
				70.391

Table 2. Optimized geometric parameters of compound 4b

Bond Length(Å)		Bond Angles (°)		Dihedral Angles (°)	
R(1,4)	1.350	A(4,1,47)	124.111	D(48,1,4,50)	178.992
R(1,47)	1.780	A(4,1,48)	123.946	D(4,1,48,3)	157.471
R(1,48)	1.780	A(47,1,48)	111.933	D(41,2,3,48)	172.998
R(2,3)	1.357	A(3,2,41)	125.758	D(3,2,41,17)	122.957
R(2,41)	1.766	A(3,2,47)	116.404	D(41,2,47,1)	171.881
R(2,47)	1.790	A(41,2,47)	117.494	D(1,4,50,5)	171.110
R(3,40)	1.766	A(6,5,50)	118.885	D(50,5,6,42)	173.968
R(3,48)	1.790	A(7,5,50)	116.915	D(5,6,42,45)	130.498
R(9,14)	1.097	A(35,33,36)	106.045	D(42,6,49,4)	179.991
R(12,15)	1.099	A(2,41,17)	101.846	D(11,8,9,13)	61.671
R(17,18)	1.530	A(6,42,43)	108.337	D(11,8,9,14)	178.131
R(17,19)	1.094	A(1,47,2)	94.577	D(14,9,12,16)	179.633
R(26,27)	1.531	A(1,48,3)	94.569	D(20,17,18,23)	178.149
R(26,28)	1.098	A(4,49,6)	95.047	D(41,17,18,21)	179.908
R(26,29)	1.098	A(4,50,5)	94.580	D(18,17,41,2)	177.453

Table 3. Optimized geometric parameters of compound 4c

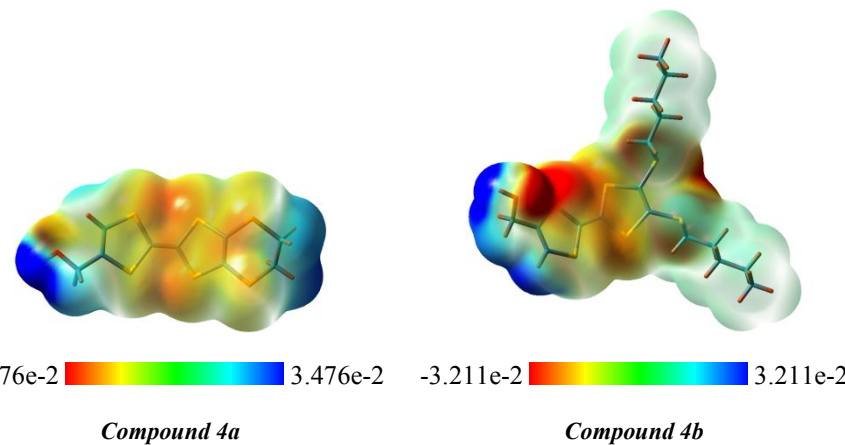
Bond Length(Å)		Bond Angles (°)		Dihedral Angles (°)	
R(1,4)	1.350	A(4,1,15)	124.153	D(16,1,4,18)	179.071
R(1,15)	1.780	A(4,1,16)	123.962	D(4,1,16,3)	156.561
R(1,16)	1.780	A(15,1,16)	111.877	D(9,2,3,16)	172.835
R(2,3)	1.356	A(3,2,9)	125.620	D(3,2,9,23)	124.310
R(2,9)	1.766	A(3,2,15)	116.401	D(9,2,15,1)	171.556
R(2,15)	1.790	A(9,2,15)	117.613	D(1,4,18,5)	171.081
R(3,8)	1.766	A(3,8,19)	101.653	D(18,5,6,10)	174.007
R(3,16)	1.790	A(2,9,23)	101.760	D(5,6,10,13)	130.637
R(4,17)	1.784	A(6,10,11)	108.323	D(17,6,10,12)	67.214
R(4,18)	1.786	A(6,10,12)	108.892	D(10,6,17,4)	179.980
R(10,13)	1.422	A(6,10,13)	109.306	D(3,8,19,22)	64.421
R(13,14)	0.966	A(11,10,12)	107.423	D(2,9,23,24)	58.510
R(19,21)	1.091	A(10,13,14)	107.948	D(2,9,23,25)	177.095
R(19,22)	1.091	A(21,19,22)	110.255	D(6,10,13,14)	163.383
R(23,24)	1.091	A(9,23,24)	111.337	D(12,10,13,14)	43.401

Table 4. Optimized geometric parameters of compound 4d

Bond Length (Å)	Bond Angles (°)	Dihedral Angles (°)
R(1,4) 1.350	A(4,1,12) 123.621	D(12,1,4,14) 177.572
R(1,12) 1.779	A(4,1,13) 123.438	D(4,1,12,2) 167.585
R(1,13) 1.779	A(12,1,13) 112.935	D(12,2,3,16) 178.628
R(2,3) 1.345	A(3,2,12) 116.984	D(3,2,20,23) 124.593
R(2,12) 1.784	A(3,2,20) 127.958	D(16,3,13,1) 172.979
R(2,20) 1.502	A(12,2,20) 115.046	D(13,3,16,18) 173.914
R(3,13) 1.784	A(7,6,14) 114.897	D(1,4,14,6) 165.210
R(3,16) 1.503	A(6,7,8) 109.950	D(15,5,6,7) 176.745
R(4,14) 1.779	A(7,10,11) 108.046	D(24,5,6,14) 177.991
R(6,7) 1.501	A(1,12,2) 95.570	D(24,5,15,4) 171.423
R(7,10) 1.425	A(1,13,3) 95.552	D(6,5,24,26) 108.935
R(10,11) 0.965	A(3,16,17) 110.882	D(15,5,24,25) 167.907
R(16,17) 1.096	A(3,16,18) 111.448	D(5,6,7,10) 135.708
R(16,18) 1.091	A(5,24,25) 111.494	D(6,7,10,11) 155.594
R(20,21) 1.096	A(4,1,12) 123.621	D(9,7,10,11) 36.076

Molecular Electrostatic Potential (MEP)

In the present study, molecular electrostatic potential (MEP) of monohydroxymethyl-TTFs **4a-d** is illustrated in Figure 2. The MEP which is a plot of electrostatic potential mapped onto the constant electron density surface. In the majority of the MEPs, while the maximum negative region which preferred site for electrophilic attack indications as red colour, the maximum positive region which preferred site for nucleophilic attack symptoms as blue colour. The importance of MESP lies in the fact that it simultaneously displays molecular size, shape as well as positive, negative and neutral electrostatic potential regions in terms of colour grading and is very useful in research of molecular structure with its physiochemical property relationship [25-27]. The resulting surface simultaneously displays molecular size and shape and electrostatic potential value. The different values of the electrostatic potential are represented by different colors. Potential increases in the order red < orange < yellow < green < blue, where blue indicates the strongest attraction and red indicates the strongest repulsion. Regions of negative V(r) are usually associated with the lone pair of electronegative atoms. As can be seen from the MEP map of the title molecules, while regions having the negative potential are over the electronegative atom (O), the regions having the positive potential are over the hydrogen atoms of hydroxyl group.



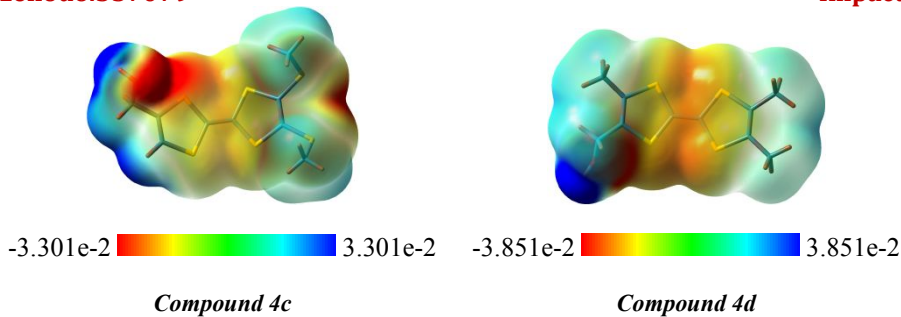


Figure 2. Molecular electrostatic potential surface of monohydroxymethyl-TTFs 4a-d

Frontier Molecular Orbitals (FMOs)

The frontier orbital's gap determines the way a molecule interacts with other species. The chemical reactivity and kinetic stability of a molecule largely depend on the energy gap between the highest occupied molecular orbital (HOMO) and the lowest unoccupied molecular orbital (LUMO). Lower the frontier orbital gap, softer and more polarizable is the molecule having high chemical-reactivity and low kinetic stability. In present study, the energies of frontier orbitals were computed in gas phase (Table 5), and the predicted shapes of FMOs are given in Figure 3. HOMO is distributed uniformly almost over the core TTF having bonding character while LUMO is found to be spread over the atoms in both ring and reflects high anti-bonding nature. The nodes of HOMOs and LUMOs are almost placed symmetrically.

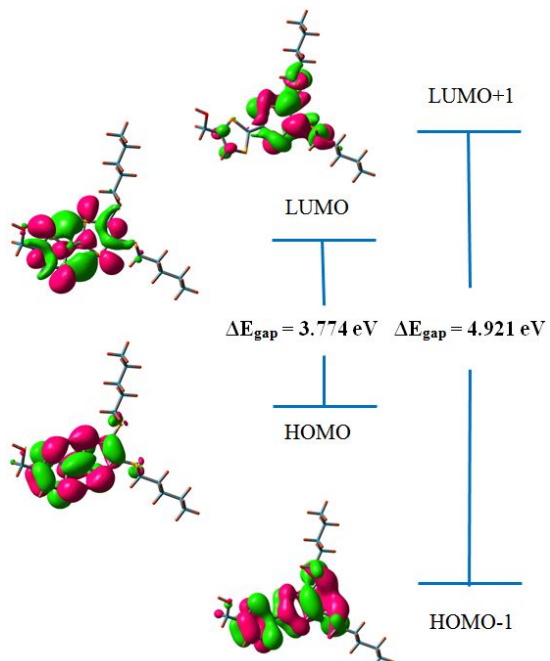


Figure 3. HOMO-LUMO Structure with the energy level diagram of compound 4b

Global Reactivity Descriptors

The energy gap between HOMO and LUMO is a critical parameter to determine molecular electrical transport properties. By using HOMO and LUMO energy values for a molecule, the global chemical reactivity descriptors of molecules such as hardness (η), chemical potential (μ), softness (S), electronegativity (χ) and electrophilicity index (ω) have been defined [28,29]. On the basis of E_{HOMO} and E_{LUMO} , these are calculated using the below equations. Using Koopman's theorem [10] for closed-shell molecules, the hardness of the molecule is

$$\eta = \frac{(I - A)}{2}$$

The chemical potential of the molecule is

$$\mu = -\frac{(I + A)}{2}$$

The softness of the molecule is

$$S = \frac{1}{2\eta}$$

The electro negativity of the molecule is

$$\chi = \frac{(I + A)}{2}$$

The electrophilicity index of the molecule is

$$\omega = \frac{\mu^2}{2\eta}$$

where (I) is the ionization potential and (A) is the electron affinity of the molecule. I and A can be expressed through HOMO and LUMO orbital energies as I = -E_{HOMO} and A = -E_{LUMO}.

Table 5. Quantum chemical descriptors of monohydroxymethyl-TTFs 4a-d

Parameters	4a	4b	4c	4d
E _{HOMO} (eV)	- 4.657	- 4.635	- 4.714	4.376
E _{LUMO} (eV)	- 0.948	- 0.861	- 0.928	- 0.690
ΔE _{gap} (eV)	3.709	3.774	3.786	3.686
IE (eV)	4.657	4.635	4.714	4.376
EA (eV)	0.948	0.861	0.928	0.690
μ (eV)	- 2.803	- 2.748	- 2.821	- 2.533
χ (eV)	2.803	2.748	2.821	2.533
η (eV)	1.855	1.887	1.893	1.843
S (eV)	0.270	0.265	0.264	0.271
ω (eV)	2.118	2.001	2.102	1.741

Local Reactivity Descriptors

Using Hirschfeld population analysis of neutral, cation and anion state of molecule, Fukui functions are calculated by following equation [30-33].

$$f^+ = [q(N+1) - q(N)], \text{ for nucleophilic attack,}$$

$$f^- = [q(N) - q(N-1)], \text{ for electrophilic attack,}$$

$$f^0 = [q(N+1) - q(N-1)]/2, \text{ for radical attack.}$$

Where, q is the gross charge of atom k in the molecule and N, N + 1, N - 1 are electron systems containing neutral, anion, cation form of molecule respectively. Where +, -, 0 signs show nucleophilic, electrophilic and radical attack respectively. Fukui functions for selected atomic sites in **4a-d** are shown in Tables 6 and 7.

Table 6. Order of the reactive sites on compounds 4a and 4b

Compound 4a					Compound 4b				
Atom	23 O	14 C	17 C	4 C	Atom	3 C	6 C	4 C	17 C
f⁺	-0.024	-0.052	-0.062	-0.049	f⁺	0.053	0.036	0.016	0.015
Atom	20 C	4 C	11 C	6 S	Atom	1 C	42 C	21 C	26 C
f⁻	-0.045	-0.049	-0.051	-0.051	f⁻	0.069	-0.002	-0.010	-0.013
Atom	23 O	14 C	17 C	4 C	Atom	1 C	3 C	6 C	4 C
f⁰	-0.025	-0.044	-0.055	-0.056	f⁰	0.039	0.013	-0.001	-0.007

Table 7. Order of the reactive sites on compounds 4c and 4d

Compound 4c					Compound 4d				
Atom	3 C	6 C	4 C	1 C	Atom	6 C	5 C	2 C	3 C
f⁺	0.057	0.038	0.020	0.005	f⁺	0.038	0.009	0.007	0.007
Atom	2 C	1 C	10 C	4 C	Atom	4 C	1 C	5 C	3 C
f⁻	0.147	0.104	-0.006	-0.012	f⁻	0.005	0.007	0.009	0.007
Atom	2 C	1 C	4 C	6 C	Atom	4 C	1 C	5 C	3 C
f⁰	0.065	0.054	0.004	-0.002	f⁰	0.024	0.018	0.012	0.007

Natural Bond Orbital Analysis (NBO)

A useful aspect of the NBO method is that it gives information about interactions in both filled and virtual orbital spaces that could enhance the analysis of intra- and intermolecular interactions. The second-order Fock matrix was calculated to evaluate the donor-acceptor interactions in NBO analysis [34]. The interactions result in a loss of occupancy from the localized NBO of the idealized Lewis structure into an empty non-Lewis orbital. For each donor (i) and acceptor (j), the stabilization energy E(2) associated with the delocalization i - j is estimated as

$$E(2) = \Delta E_{ij} = q_i \frac{F^2(i,j)}{E_j - E_i}$$

Where q_i is the donor orbital occupancy, E_i and E_j are diagonal elements and F_{ij} is the off diagonal NBO Fock matrix element. NBO analysis gives a convenient basis for investigating charge transfer or conjugative interaction in molecular systems. Some electron donor orbital, acceptor orbital and the interacting stabilization energies resulting from the second-order micro-disturbance theory are reported [35,36]. The larger the E(2) value, the more intensive is the interaction between electron donors and electron acceptors, i.e., the more donating tendency from electron donors to electron acceptors and the greater the extent of conjugation of the whole system. Delocalization of electron density between occupied Lewis-type (bond or lone pair) NBO orbital and formally unoccupied (antibond or Rydberg) non-Lewis NBO orbital correspond to a stabilizing donor-acceptor interaction. NBO analysis was performed on the title molecules at B3LYP/6-31G(d,p) level in order to elucidate the intramolecular, hybridization and delocalization of electron density in the molecule. Hybrids of natural bond orbitals calculated by NBO analysis are given in Tables 8-11.

Table 8. Second order perturbation theory analysis of Fock matrix on NBO of compound 4a

Donor(i)	ED/e	Acceptor(j)	ED/e	E(2) Kcal/mol	E(j)-E(i) a.u	F(i,j) a.u
LP(2)S5	1.77614	$\pi^*(C3-C4)$	0.22411	21.08	0.27	0.067
LP(2)S6	1.78735	$\pi^*(C3-C4)$	0.22411	20.66	0.27	0.067
LP(2)S7	1.80037	$\pi^*(C10-C11)$	0.36650	19.49	0.24	0.063
LP(2)S8	1.80038	$\pi^*(C10-C11)$	0.36650	19.46	0.24	0.063
LP(2)S5	1.77614	$\pi^*(C1-C2)$	0.38035	17.16	0.26	0.062
LP(2)S13	1.85761	$\pi^*(C10-C11)$	0.36650	17.03	0.24	0.060
LP(2)S6	1.78735	$\pi^*(C1-C2)$	0.38035	16.58	0.26	0.061
LP(2)S8	1.80038	$\pi^*(C1-C2)$	0.38035	12.58	0.26	0.053
LP(2)S7	1.80037	$\pi^*(C1-C2)$	0.38035	12.39	0.26	0.053
LP(2)S12	1.87554	$\pi^*(C10-C11)$	0.36650	10.08	0.24	0.047
LP(2)O23	1.96081	$\sigma^*(C20-H22)$	0.03087	7.90	0.73	0.068
$\sigma(C4-H9)$	1.97197	$\sigma^*(C3-S6)$	0.03154	6.46	0.74	0.062
$\pi^*(C1-C2)$	0.38035	$\sigma^*(C1-C2)$	0.04246	6.01	0.58	0.115
$\sigma(S8-C10)$	1.97041	$\sigma^*(C11-S13)$	0.03021	5.60	0.84	0.061
$\sigma(S7-C11)$	1.96873	$\sigma^*(C10-S12)$	0.02956	5.31	0.84	0.060
$\sigma(C1-S7)$	1.97013	$\sigma^*(C2-S6)$	0.04096	5.11	0.82	0.058
$\sigma(C2-S6)$	1.97261	$\sigma^*(C1-S7)$	0.04516	5.09	0.83	0.058
$\sigma(C2-S5)$	1.97319	$\sigma^*(C1-S8)$	0.04467	5.08	0.83	0.058
$\sigma(C1-S8)$	1.97049	$\sigma^*(C2-S5)$	0.04297	5.02	0.82	0.058
$\sigma(C17-H18)$	1.97374	$\sigma^*(S13-C14)$	0.03110	5.02	0.66	0.052

Table 9. Second order perturbation theory analysis of Fock matrix on NBO of compound 4b

Donor(i)	ED/e	Acceptor(j)	ED/e	E(2) Kcal/mol	E(j)-E(i) a.u	F(i,j) a.u
LP(2)S49	1.77635	$\pi^*(C_5-C_6)$	0.22782	21.47	0.26	0.067
LP(2)S50	1.77474	$\pi^*(C_5-C_6)$	0.22782	21.22	0.27	0.067
LP(2)S48	1.79251	$\pi^*(C_2-C_3)$	0.31224	19.19	0.25	0.063
LP(2)S47	1.79372	$\pi^*(C_2-C_3)$	0.31224	19.12	0.25	0.063
LP(2)S49	1.77635	$\pi^*(C_1-C_4)$	0.38235	17.54	0.26	0.063
LP(2)S50	1.77474	$\pi^*(C_1-C_4)$	0.38235	16.82	0.26	0.062
LP(2)S48	1.79251	$\pi^*(C_1-C_4)$	0.38235	13.12	0.26	0.054
LP(2)S47	1.79372	$\pi^*(C_1-C_4)$	0.38235	13.06	0.26	0.054
LP(2)O45	1.95602	$\sigma^*(C_{42}-H_{43})$	0.02798	8.23	0.74	0.070
$\pi^*(C_1-C_4)$	0.38235	$\sigma^*(C_1-C_4)$	0.04169	6.09	0.59	0.116
$\sigma(C_5-H_7)$	1.97425	$\sigma^*(C_6-S_{49})$	0.03720	6.08	0.75	0.060
$\sigma(C_{42}-H_{43})$	1.98166	$\sigma^*(C_6-S_{49})$	0.03720	5.62	0.72	0.057
$\sigma(C_2-S_{47})$	1.97161	$\sigma^*(C_3-S_{40})$	0.03072	5.41	0.84	0.060
$\sigma(C_3-S_{48})$	1.97159	$\sigma^*(C_2-S_{41})$	0.03084	5.41	0.84	0.060
$\sigma(C_4-S_{49})$	1.97250	$\sigma^*(C_1-S_{47})$	0.04561	5.15	0.83	0.059
$\sigma(C_4-S_{50})$	1.97316	$\sigma^*(C_1-S_{48})$	0.04585	5.13	0.83	0.059
LP(2)S40)	1.88677	$\sigma^*(C_2-C_3)$	0.05101	5.13	0.81	0.058
$\sigma(C_1-S_{48})$	1.97080	$\sigma^*(C_4-S_{50})$	0.04409	5.07	0.82	0.058
$\sigma(C_1-S_{47})$	1.97112	$\sigma^*(C_4-S_{49})$	0.04114	5.01	0.82	0.057
LP(2)S41)	1.88498	$\sigma^*(C_2-C_3)$	0.05101	4.97	0.81	0.057

Table 10. Second order perturbation theory analysis of Fock matrix on NBO of compound 4c

Donor(i)	ED/e	Acceptor(j)	ED/e	E(2) Kcal/mol	E(j)-E(i) a.u	F(i,j) a.u
LP(2)S17	1.77493	$\pi^*(C5-C6)$	0.22740	21.47	0.26	0.067
LP(2)S18	1.77353	$\pi^*(C5-C6)$	0.22740	21.21	0.27	0.067
LP(2)S16	1.79397	$\pi^*(C2-C3)$	0.31236	19.18	0.25	0.063
LP(2)S15	1.79534	$\pi^*(C2-C3)$	0.31236	19.08	0.25	0.063
LP(2)S17	1.77493	$\pi^*(C1-C4)$	0.38196	17.77	0.26	0.063
LP(2)S18	1.77353	$\pi^*(C1-C4)$	0.38196	17.04	0.26	0.062
LP(2)S16	1.79397	$\pi^*(C1-C4)$	0.38196	12.82	0.26	0.054
LP(2)S15	1.79534	$\pi(C1-C4)$	0.38196	12.77	0.26	0.054
LP(2)O13	1.95592	$\sigma^*(C10-H11)$	0.02798	8.23	0.74	0.070
$\sigma(C5-H7)$	1.97420	$\sigma^*(C6-S17)$	0.03729	6.08	0.75	0.060
$\pi^*(C1-C4)$	0.38196	$\sigma^*(C1-C4)$	0.04153	5.92	0.59	0.114
$\sigma(C10-H11)$	1.98159	$\sigma^*(C6-S17)$	0.03729	5.63	0.72	0.057
$\sigma(C2-S15)$	1.97166	$\sigma^*(C3-S8)$	0.03381	5.39	0.84	0.060
$\sigma(C3-S16)$	1.97164	$\sigma^*(C2-S9)$	0.03391	5.39	0.84	0.060
$\sigma(C4-S17)$	1.97248	$\sigma^*(C1-S15)$	0.04534	5.15	0.83	0.059
$\sigma(C4-S18)$	1.97312	$\sigma^*(C1-S16)$	0.04553	5.15	0.83	0.059
$\sigma(C1-S16)$	1.97073	$\sigma^*(C4-S18)$	0.04401	5.05	0.82	0.058
$\sigma(C1-S15)$	1.97104	$\sigma^*(C4-S17)$	0.04110	4.99	0.82	0.057
LP(2)S8)	1.88336	$\sigma(C2-C3)$	0.05083	4.93	0.81	0.057
LP(2)S9)	1.88218	$\sigma^*(C2-C3)$	0.05083	4.84	0.81	0.057

Table 11. Second order perturbation theory analysis of Fock matrix on NBO of compound 4d

Donor(i)	ED/e	Acceptor(j)	ED/e	E(2) Kcal/mol	E(j)-E(i) a.u	F(i,j) a.u
LP(2)S15	1.79438	$\pi^*(C5-C6)$	0.23467	20.02	0.27	0.066
LP(2)S13	1.79694	$\pi^*(C2-C3)$	0.23340	19.64	0.27	0.066
LP(2)S12	1.79762	$\pi(C2-C3)$	0.23340	19.51	0.27	0.065
LP(2)S14	1.79253	$\pi(C5-C6)$	0.23467	19.08	0.26	0.064
LP(2)S13	1.79694	$\pi^*(C1-C4)$	0.38307	15.76	0.26	0.060
LP(2)S12	1.79762	$\pi^*(C1-C4)$	0.38307	15.73	0.26	0.060
LP(2)S14	1.79253	$\pi^*(C1-C4)$	0.38307	15.47	0.26	0.059
LP(2)S15	1.79438	$\pi(C1-C4)$	0.38307	15.08	0.26	0.059
LP(2)O10	1.95321	$\sigma^*(C7-H8)$	0.02913	7.82	0.75	0.069
$\pi^*(C1-C4)$	0.38307	$\sigma^*(C1-C4)$	0.04232	6.81	0.58	0.122
$\sigma(C5-S15)$	1.97190	$\sigma^*(C6-C7)$	0.03138	5.29	1.04	0.066
$\sigma(C2-S12)$	1.97154	$\sigma^*(C3-C16)$	0.01857	5.21	1.04	0.066
$\sigma(C3-S13)$	1.97146	$\sigma^*(C2-C20)$	0.01859	5.21	1.04	0.066
$\sigma(C4-S14)$	1.97197	$\sigma^*(C1-S12)$	0.03975	5.16	0.83	0.058
$\sigma(C6-S14)$	1.97024	$\sigma^*(C5-C24)$	0.01861	5.15	1.03	0.065
$\sigma(C2-C20)$	1.97884	$\sigma^*(C2-C3)$	0.02960	5.14	1.29	0.073
$\sigma(C3-C16)$	1.97878	$\sigma(C2-C3)$	0.02960	5.14	1.29	0.073
$\sigma(C4-S15)$	1.97315	$\sigma^*(C1-S13)$	0.03956	5.13	0.83	0.058
$\sigma(C1-S13)$	1.97300	$\sigma(C4-S15)$	0.04084	5.12	0.83	0.058
$\sigma(C5-C24)$	1.97917	$\sigma^*(C5-C6)$	0.02881	5.07	1.29	0.072

Nonlinear Optical Properties (NLO)

Hyperpolarizabilities are very sensitive to the basis sets and level of theoretical approach employed [37-39], that the electron correlation can change the value of hyperpolarizability. Urea is one of the prototypical molecules used in the study of the nonlinear optical (NLO) properties of molecular systems. Therefore it has been used frequently as a threshold value for comparative purposes. The calculations of the total molecular dipole moment (μ), linear polarizability (α) and first-order hyperpolarizability (β_{tot}) from the Gaussian output have been explained in detailed previously [19] and DFT has been extensively used an effective method to investigate the organic NLO material

[20]. The polar properties of the title compounds were calculated by Density Functional Theory (DFT) using B3LYP method with 6-31G(d,p) basis set using Gaussian 09W program package. The total molecular dipole moments of monohydroxymethyl-TTFs **4a-d** from B3LYP basis set are collected in Table 12. The total molecular dipole moment of compounds **4a-d** from B3LYP/6-31G(d,p) basis set are 1.584D, 4.336D, 4.506D and 2.723D respectively, which are the four times greater than the value of urea ($\mu = 1.3732\text{D}$). Similarly the first order hyperpolarizability of the title molecules is $2.964 \times 10^{-30} \text{ esu}$ that value is seven times greater than the value of urea ($\beta_{\text{tot}} = 0.372 \times 10^{-30} \text{ esu}$). From the magnitude of first hyperpolarizability, the monohydroxymethyl-TTFs **4a-d** may be a potential applicant in the dipole moment of NLO materials.

Table 12. The dipole moments μ (D), polarizability α (esu), anisotropy of the polarizability $\Delta\alpha$ (esu), and the first hyperpolarizability β (esu) of monohydroxymethyl-TTFs 4a-d

Parameters	5a	5b	5c	5i
β_{xxx}	-50.7172	-316.9206	-263.6682	-30.3900
B_{yyy}	-0.0837	27.8706	28.3039	-24.1309
B_{zzz}	4.6707	23.8060	16.0279	4.4937
B_{xyy}	-36.1531	-8.5950	-5.0889	-27.6470
B_{xxy}	-70.4794	-53.6246	21.6480	-24.2213
B_{xxz}	41.9744	102.8024	37.4586	50.2029
B_{xzz}	-13.6599	-18.4770	14.8209	-6.8691
B_{yzz}	-3.8698	-1.2422	0.0653	-2.9287
B_{yyz}	2.7918	26.5663	27.4171	8.7384
B_{xyz}	10.3907	17.1192	2.6466	12.1937
$B_{tot}(\text{esu}) \times 10^{-33}$	901.9195455	2964.50903	810.4801759	737.2317287
μ_x	0.0631	-2.1916	-3.8191	-0.4261
μ_y	-1.5448	-0.2333	0.1524	-0.1729
μ_z	0.3468	3.7349	2.3881	2.6845
$\mu_{tot} (\mathbf{D})$	1.584505882	4.33670583	4.506858349	2.7235998
α_{xx}	-85.6651	-147.7380	-108.0493	-81.8013
α_{yy}	-137.3282	-174.9504	-126.7587	-111.7872
α_{zz}	-138.9779	-197.7637	-139.0479	-120.9381
α_{xy}	7.9164	3.0362	-2.4074	0.2115
α_{xz}	-10.4841	-3.5309	8.7339	-6.7280
α_{yz}	-0.9368	-2.2999	-1.6816	-3.0242
$\alpha (\text{esu}) \times 10^{-24}$	-16.54757728	-25.71033374	-18.46848146	-15.53761404
$\Delta\alpha(\text{esu}) \times 10^{-24}$	8.48426043	6.56559776	4.65287284	5.58590286

IV. CONCLUSION

In conclusion, based on the density functional theory B3LYP/6-31G(d,p) method, The optimized geometric parameters (bond lengths and bond angles) are theoretically determined. Various properties like structure geometry , non-linear optical (NLO) property, Natural Bond Orbital (NBO), Highest Occupied Molecular Orbital (HOMO), lowest unoccupied molecular orbital (LUMO) energies and Molecular Electrostatic Potential (MEP) analysis of the monohydroxymethyl-TTFs are performed to elucidate the information regarding charge transfer within the molecules.

This work was generously supported by the (General Directorate for Scientific Research and Technological Development, DGRS-DT) and Algerian Ministry of Scientific Research

REFERENCES

1. P.Batail, "Introduction: Molecular Conductors", *Chem. Rev.* 2004; 104:4887-4890.
2. J.Jeppesen, O.Becher, "Pyrrolo-tetrathiafulvalenes and their applications in molecular and supramolecular chemistry", *J. Eur. J. Org. Chem.* 2003; 3245-3266.
3. C.Jia, S.-X.Liu,C.Tanner,C.Leiggner, A.Neels, L.Sanguinet, E.Levillain, S.Leutwyler, A.Hauser, S.Decurtins, "An experimental and computational study on intramolecular charge transfer: A tetrathiafulvalene-fused dipyridophenazine molecule", *Chem. Eur. J.* 2007; 13:3804-3812.
4. K. S.Gavrilenko, Y.Le Gal, O.Cador, S.Golhen, L.Ouahab, "First trinuclear paramagnetic transition metal complexes with redox active ligands derived from TTF: Co₂M(PhCOO)₆(TTF-CH[double bond, length as m-dash]CH-py)2•2CH₃CN, M = Co^{II}, Mn^{II}", *Chem. Commun.* 2007; 280-282.
5. J.Massue,N.Bellec, S.Chopin, E.Levillain, T.Roisnel, R.Clerac, D.Lorcy, "Electroactive ligands: The first metal complexes of tetrathiafulvenyl-acetylacetone", *Inorg. Chem.* 2005; 44:8740-8748.
6. M.Guerro, T.Roisnel, P.Pellon, D.Lorcy, "Redox-active dithiafulvenyldiphenylphosphine as a mono or bidentate ligand: Intramolecular coupling reaction in the coordination sphere of a metal carbonyl fragment", *Inorg. Chem.* 2005; 44:3347-3355.
7. J.-C.Wu, S.X.Liu, A.Neels, F.Le Derf, M.Salle, S.Decurtins, "A tetrathiafulvalene-tetracyanoanthraquinodimethane (TTF-TCNAQ) diad with a chemically tunable HOMO-LUMO gap", *Tetrahedron* 2007; 63:11282-11286.
8. D.R. Kanis, M.A. Ratner, T. Marks, "Design and construction of molecular assemblies with large second-order optical nonlinearities Quantum chemical aspects", *J. Chem. Rev.* 1994; 94:195-242.
9. P.N. Prasad, D.J. Williams, "Introduction to nonlinear optical effects in molecules and polymers", Wiley, New York, 1991.
10. H. Tanak, "Crystal structure, spectroscopy and quantum chemical", *Int. J. Quant. Chem.* 2012; 112:2392-2402.
11. S.R. Marder, B. Kippelen, A.K.Y. Jen, N. Peyghambarian, "Design and synthesis of chromophores and polymers for electro-optic and photorefractive applications", *Nature* 1997; 388:845-851.
12. H. Ikeda, T. Sakai, K. Kawasaki, "Nonlinear optical properties of cyanine dyes", *Chem. Phys. Lett.* 1991; 179 :551-554.
13. H.E. Katz, K.D. Singer, J.E. Sohn, C.W. Dirk, L.A. King, H.M. Gordon, "Greatly enhanced second-order nonlinear optical susceptibilities in donor-acceptor organic molecules", *J. Am. Chem. Soc.* 1987; 109:6561-6563.
14. D. Sajan, H. Joe, V.S. Jayakumar, J. Zaleski, "Structural and electronic contributions to hyperpolarizability in methyl p-hydroxy benzoate", *J. Mol. Struct.* 2006; 785:43-53.
15. J.E. Rice, N.C. Handy, "The calculation of frequency-dependent polarizabilities as pseudo-energy derivatives", *J. Chem. Phys.* 1991; 94:4959-4971.
16. H. Li, K. Han, X. Shen, Z. Lu, Z. Huang, W. Zhang, Z. Zhang, L. Bai, "The first hyperpolarizabilities of hemicyanine cationic derivatives studied by finite-field (FF) calculations", *J. Mol. Struct. Theochem.* 2006; 767:113-118.
17. H.L. Xu, Z.R. Li, D. Wu, B.Q. Wang, Y. Li, F.L. Gu, Y. Aoki, "Structures and Large NLO responses of new electrides: Li-doped fluorocarbon chain", *J. Am. Chem. Soc.* 2007; 129:2967-2970.
18. D. Avci, A. Basoglu, Y. Atalay, "Ab initio HF and DFT calculations on an organic non-linear optical material", *Struct. Chem.* 2010; 21:213-219.
19. M. Toy, H. Tanak, "DFT quantum chemical studies on 1-[n-(2-pyridyl) aminomethylidene]-2(1h)-napthalenone", *J. Theo. Comput. Chem.* 2012; 11:745-762.
20. C. Carcel, L. Kaboub, A.K. Gouasmia, J.M. Fabre, "Synthesis and redox properties of several new oligo TTF containing functional spacer", *Synthetic Metals* 2006; 156:1271-1279.

21. H.Muller, A.Lerf, H. P.Fritz, K.Andres, "Some new applications of thiapendione and synthesis of bis-(phenylenedithiolo)-tetrathiafulvalene", *Synthetic Metals*, 1991; 42:2381-2384.
22. S.Yoneda, T.Kawase, Y.Yasuda, z.Yoshida, "New syntheses of tetrathiafulvalene". *J. Org. Chem.*, 1979; 44:1728-1729.
23. H. K.Spencer, M. P.Cava, A. F. Garito,« Organic metals: Synthesis of benzotetrathiafulvalene", *J. Chem. Soc., Chem. Commun*, 1976, 966-967.
24. M. V.Lakshminikantham, M. P.Cava, "Alternate synthesis of tetraselenafulvalene". *J. Org. Chem.*, 1976. 41:882-882.
25. J.S. Murray, K. Sen, "Molecular electrostatic potentials: concepts and applications", vol. 399, Elsevier, Amsterdam, 1996, p. 400.
26. E. Scrocco, J. Tomasi, in: P. Lowdin, "Advances in quantum chemistry", vol. 402, Academic Press, New York, 1978, p. 403.
27. J. Sponer, P. Hobza, "DNA base amino groups and their role in molecular interactions: Ab initio and preliminary density functional theory calculations", *Int. J. Quant. Chem.* 1996; 57:959-970.
28. R. Parr, L. Szentpaly, S. Liu, "Electrophilicity index", *Am. Chem. Soc.* 1999; 121:1922-1924.
29. P. Chattraj, B. Maiti, U. Sarkar, "Philicity: A unified treatment of chemical reactivity and selectivity", *J. Phys. Chem. A* 2003; 107:4973-4975.
30. L.HMendoza-Huizar, C.HRios-Reyes, "Chemical reactivity of atrazine employing the Fukui function", *J. Mex. Chem. Soc.* 2011; 55:142-147.
31. L.Komorowski, J.Lipinski, P.Szarek, P.Ordon, "Polarization justified Fukui functions: the theory and applications for molecules", *J. Chem. Phys.* 2011; 135:014109.
32. N.OEddy, E.E.OEbens, U.JIbok, E.EAkpan, "Experimental and computational chemistry studies on the inhibition of the corrosion of mild steel in H₂SO₄ by (2s,5s,6r)-6-(2-(aminomethyl)-5-(3-(2-chlorophenyl)isoxazol-5-yl)benzamido)-3,3-dimethyl-7-oxo-4-thia-1-azabicyclo[3.2.0]heptane-2-carboxylic acid". *Int. J. Electrochem. Sci.* 2011; 6:4296-4315.
33. P.KChattaraj, S.Giri, "Stability, reactivity, and aromaticity of compounds of a multivalent superatom", *J. Phys. Chem. A*. 2007; 111:11116-11121.
34. M. Szafran, A. Komasa, E.B. Adamska, "Crystal and molecular structure of 4-carboxypiperidinium chloride (4-piperidinecarboxylic acid hydrochloride)", *J. Mol. Struct.* 2007; 827:101-107.
35. T. Vijayakumar, I. HubertJoe, C.P.R. Nair, V.S. Jayakumar, "Efficient π electrons delocalization in prospective push-pull non-linear optical chromophore 4-[N, N-dimethylamino]-4'-nitro stilbene (DANS): A vibrational spectroscopic study", *J. Chem. Phys.* 2008; 343:83-89.
36. R.S. Mulliken, "Electronic population analysis on LCAO-MO molecular wave functions", *J. Chem. Phys.* 1955; 23:1833-1840.
37. A.E. Reed, L.A. Curtiss, F. Weinheld, "Intermolecular interactions from a natural bond orbital, donor-acceptor viewpoint", *Chem. Rev.* 1988; 88:899-926.
38. J.P. Foster, F. Weinhold, "Natural hybrid orbitals", *J. Am. Chem. Soc.* 1980; 102:7211-7218.
39. H. Sekino, R.J. Bartlett, "Hyperpolarizabilities of the hydrogen fluoride molecule: A discrepancy between theory and experiment", *J. Chem. Phys.* 1986; 84:2726-2733